

# Measurements of the $WW$ and combined $WW/WZ$ production cross sections in $\sqrt{s} = 7$ TeV $pp$ collisions with the ATLAS detector and limits on anomalous triple gauge couplings

---

Jianbei Liu<sup>\*†</sup>

*on behalf of the ATLAS Collaboration*

*University of Science and Technology of China*

*E-mail: [jianbei.liu@cern.ch](mailto:jianbei.liu@cern.ch)*

A measurement of the  $WW$  production cross section using the  $WW$  fully leptonic decays in  $4.64 \text{ fb}^{-1}$  of 7 TeV  $pp$  collisions recorded with the ATLAS detector at the large hadron collider is presented. The measured total cross section is  $\sigma(pp \rightarrow WW) = 51.9 \pm 2.0$  (stat.)  $\pm 3.9$  (syst.)  $\pm 0.9$  (lumi.) pb, consistent with the Standard Model prediction of  $44.7 \pm 2.8$  pb. The normalized  $WW$  production cross section within a fiducial phase space is also measured as a function of the leading lepton transverse momentum. Limits on anomalous triple gauge couplings are derived based on the leading lepton transverse momentum distribution in the  $WW$  leptonic decay events. Also presented is a measurement of the combined  $WW$  and  $WZ$  production cross section using their experimentally undistinguishable common semi-leptonic final state of  $lvq\bar{q}$  with the same dataset. The combined cross section is measured to be  $\sigma(WW + WZ) = 72 \pm 9$  (stat.)  $\pm 15$  (syst.  $\oplus$  lumi.)  $\pm 13$  (MC stat.) pb, compatible with the Standard Model expectation of  $63.4 \pm 2.6$  pb.

*The European Physical Society Conference on High Energy Physics -EPS-HEP2013*

*18-24 July 2013*

*Stockholm, Sweden*

---

<sup>\*</sup>Speaker.

<sup>†</sup>Phys. Rev. D 87, 112001 (2013); ATLAS-CONF-2012-157

## 1. Introduction

The production of vector gauge boson pairs (diboson production) in pp collisions at the large hadron collider (LHC) [1] offers an important testing ground for the electroweak sector of the Standard Model (SM). In the SM, the triple gauge couplings (TGC) between vector bosons are completely fixed by the non-Abelian electroweak gauge structure of  $SU(2)_L \times U(1)_Y$ . The production rate and kinematic distributions of vector boson pairs are therefore well predicted in the SM. Anomalous triple gauge boson couplings (aTGC) beyond the SM gauge constraints or new high mass resonances decaying into a vector boson pair could alter the triple gauge vertices causing deviations of diboson production rate and kinematic distributions from their SM predictions [2] [3]. Therefore, precision measurements of diboson production allow a direct test of the electroweak theory and are sensitive probes of new physics beyond the SM in the electroweak sector, complementary to direct searches. In addition, diboson production usually constitutes important backgrounds to the studies of the SM higgs and to searches for new physics beyond the SM due to sharing the same or similar final states.

The fully leptonic decays of boson pairs provide a very clean signature with low background. The semi-leptonic decays of boson pairs offer another approach to studying diboson production thanks to the significantly larger event rates. This note presents a measurement of integrated and differential WW production cross sections in fully leptonic final states and limits on anomalous triple gauge couplings. A cross section measurement of the combined WW and WZ production in their shared semi-leptonic final state is also presented. The data used in the measurements presented in this note were selected with the ATLAS detector [4] using single lepton triggers. The corresponding total integrated luminosity is  $4.6 \text{ fb}^{-1}$  with an uncertainty of 3.9%.

Previous measurements on WW production and combined WW and WZ production can be found in [5], [6], [7], [8] and [9].

## 2. WW production in fully leptonic decay channels

### 2.1 Event selection and signal acceptance

The signature of a leptonically decaying WW event is the presence of two oppositely-charged leptons (electrons or muons) with large missing transverse momentum ( $E_T^{miss}$ ) and low jet activity. The final states are accordingly classified into three flavors:  $ee$ ,  $\mu\mu$  and  $e\mu$ . An event selection is devised to fully exploit these characteristics to maximize signal to background ratio. The selection details can be found in [10]. Simulated signal WW events are passed through the event selection to determine the signal acceptance. A fiducial phase space is defined by mimicking the analysis event selection at generator level. Cross sections measured in this phase space have reduced uncertainties due to small theoretical extrapolation. The overall acceptance can be separated into two factors  $A_{WW}$  and  $C_{WW}$ , where  $A_{WW}$  represents the extrapolation from the fiducial phase space to the total phase space, while  $C_{WW}$  accounts for detector effects in the fiducial phase space. The product of  $A_{WW}$  and  $C_{WW}$  is then the overall acceptance.

Table 1 gives the estimated  $A_{WW}$  and  $C_{WW}$  factors and their products  $A_{WW} \times C_{WW}$  for all the three channels. The leading systematic uncertainty on  $A_{WW}$  arises from theoretical modeling of jet veto (5.6%). The main sources of systematic uncertainty on  $C_{WW}$  are electron efficiency (1.4%

uncertainty on  $C_{WW}$  per electron) and jet veto efficiency (2.8% uncertainty on  $C_{WW}$ ) followed by lepton  $p_T$  scale and resolution, and effects of jet energy scale and resolution on  $E_T^{miss}$ . The systematic uncertainties on  $A_{WW} \times C_{WW}$  are smaller than the corresponding quadrature sums of the uncertainties on  $A_{WW}$  and  $C_{WW}$  due to correlations in theoretical uncertainties between  $A_{WW}$  and  $C_{WW}$ .

	$ee$	$\mu\mu$	$e\mu$
$A_{WW}$	$(7.5 \pm 0.1 \pm 0.4)\%$	$(8.1 \pm 0.1 \pm 0.5)\%$	$(15.9 \pm 0.1 \pm 0.9)\%$
$C_{WW}$	$(40.3 \pm 0.5 \pm 1.7)\%$	$(68.7 \pm 0.5 \pm 2.1)\%$	$(50.5 \pm 0.2 \pm 1.6)\%$
$A_{WW} \times C_{WW}$	$(3.0 \pm 0.1 \pm 0.1)\%$	$(5.6 \pm 0.1 \pm 0.2)\%$	$(8.0 \pm 0.1 \pm 0.3)\%$

**Table 1:** Acceptance  $A_{WW}$ ,  $C_{WW}$  and  $A_{WW} \times C_{WW}$  for  $ee$ ,  $\mu\mu$  and  $e\mu$  channels [10]. The first uncertainty is statistical, the second systematic.

## 2.2 Background estimation

Background events come from  $W$ +jets production, Drell-Yan production, top production and other diboson processes.

The  $W$ +jets background is determined by using a data control sample dominated by  $W$ +jets events. The  $W$ +jets background is then estimated by scaling the control sample by a factor measured in a QCD dijet data sample. The final estimates of  $W$ +jets background are  $21 \pm 1$  (stat.)  $\pm 11$  (syst.),  $7 \pm 1$  (stat.)  $\pm 3$  (syst.), and  $70 \pm 2$  (stat.)  $\pm 31$  (syst.) for the  $ee$ ,  $\mu\mu$  and  $e\mu$  channels, respectively. A Drell-Yan dominated control region is constructed by reverting the  $p_T(l)$  cuts in the analysis event selection. The Drell-Yan estimates from simulation are then normalized to data in this control region. The final estimates of Drell-Yan background are  $12 \pm 3$  (stat.)  $\pm 3$  (syst.),  $34 \pm 6$  (stat.)  $\pm 10$  (syst.) and  $5 \pm 2$  (stat.)  $\pm 1$  (syst.) in the  $ee$ ,  $\mu\mu$  and  $e\mu$  channels, respectively. The top background arises from  $t\bar{t}$  and single top production. It is estimated by utilizing jet multiplicity in the event. The final estimates of top background are  $22 \pm 12$  (stat.)  $\pm 3$  (syst.),  $32 \pm 14$  (stat.)  $\pm 5$  (syst.) and  $87 \pm 23$  (stat.)  $\pm 13$  (syst.) for the  $ee$ ,  $\mu\mu$  and  $e\mu$  channels, respectively. The background arising from other non- $WW$  diboson processes including  $WZ/\gamma^*$ ,  $W\gamma$ ,  $Z\gamma$  and  $ZZ$  is estimated using simulation and normalized by cross sections predicted at NLO. The final estimates of this background are  $13 \pm 1$  (stat.)  $\pm 2$  (syst.),  $21 \pm 1$  (stat.)  $\pm 2$  (syst.) and  $44 \pm 2$  (stat.)  $\pm 6$  (syst.).

## 2.3 Cross section results

The numbers of expected and observed events after applying all selection cuts are shown in Table 2. In total 1325 candidate events are observed in data with  $824 \pm 4$  (stat.)  $\pm 69$  (syst.)  $WW$  signal events and  $369 \pm 31$  (stat.)  $\pm 53$  (syst.) background events.

The fiducial cross section and total cross section are calculated using these numbers together with the  $C_{WW}$  and  $A_{WW}$  factors described in Sec. 2.1 and the integrated luminosity the data sample corresponds to. The total cross sections from the three decay channels are combined by minimizing a negative log-likelihood function that takes all the correlations between channels into account properly.

Data	$ee$ 174	$\mu\mu$ 330	$e\mu$ 821	combined 1325
WW	$100 \pm 2 \pm 9$	$186 \pm 2 \pm 15$	$538 \pm 3 \pm 45$	$824 \pm 4 \pm 69$
Total background	$68 \pm 12 \pm 13$	$94 \pm 15 \pm 13$	$206 \pm 24 \pm 35$	$369 \pm 31 \pm 53$
Total expected	$169 \pm 12 \pm 16$	$280 \pm 16 \pm 20$	$744 \pm 24 \pm 57$	$1192 \pm 31 \pm 87$

**Table 2:** Summary of observed and expected numbers of signal and background events in three individual channels [10]. For each expected number, the first uncertainty is statistical and the second systematic.

Table 3 presents the fiducial and total cross sections from the three channels and the combined total cross section. Their SM predictions are also presented for comparison. The predicted cross sections are calculated at next-to-leading order (NLO) using MCFM [11] with the CT10 [12] parton distribution functions (PDFs). The calculated total cross section is  $44.7^{+2.1}_{-1.9}$  pb.

	Measured $\sigma_{WW}^{fid}$ (fb)	Predicted $\sigma_{WW}^{fid}$ (fb)	Measured $\sigma_{WW}$ (fb)	Predicted $\sigma_{WW}$ (fb)
$ee$	$56.4 \pm 6.8 \pm 9.8 \pm 2.2$	$54.6 \pm 3.7$	$46.9 \pm 5.7 \pm 8.2 \pm 1.8$	$44.7^{+2.1}_{-1.9}$
$\mu\mu$	$73.9 \pm 5.9 \pm 6.9 \pm 2.9$	$58.9 \pm 4.0$	$56.7 \pm 4.5 \pm 5.5 \pm 2.2$	$44.7^{+2.1}_{-1.9}$
$e\mu$	$262.3 \pm 12.3 \pm 20.7 \pm 10.2$	$231.4 \pm 15.7$	$51.1 \pm 2.4 \pm 4.2 \pm 2.0$	$44.7^{+2.1}_{-1.9}$
Combined	...	...	$46.9 \pm 5.7 \pm 83 \pm 1.8$	$44.7^{+2.1}_{-1.9}$

**Table 3:** The measured fiducial and total cross sections for the three channels separately and also the total cross section for the combined channels, compared with theoretical predictions. For the measured cross sections, the first uncertainty is statistical, the second is systematic without luminosity uncertainty, and the third is the luminosity uncertainty [10].

The measured leading lepton  $p_T$  distribution is unfolded with a Bayesian unfolding technique [13] to remove all detector effects. Figure 1 shows the normalized fiducial cross sections extracted in bins of the leading lepton  $p_T$  in comparison with the SM predictions. The normalized differential cross section is the normalized sum of the fiducial cross sections in the three channels.

## 2.4 Anomalous triple gauge couplings

The general Lorentz invariant Lagrangian describing the WWZ and WW $\gamma$  triple gauge interactions contains 14 independent coupling parameters [14]. Assuming electromagnetic gauge invariance and C and P conservations, the number of independent parameters reduces to five:  $g_1^Z$ ,  $\kappa^Z$ ,  $\kappa^\gamma$ ,  $\lambda^Z$ ,  $\lambda^\gamma$ . In the SM,  $g_1^Z = \kappa^Z = \kappa^\gamma = 1$  and  $\lambda^Z = \lambda^\gamma = 0$ . Deviations of these coupling parameters from their SM values:  $\delta g_1^Z (= g_1^Z - 1)$ ,  $\delta \kappa^Z (= \kappa^Z - 1)$ ,  $\delta \kappa^\gamma (= \kappa^\gamma - 1)$ ,  $\lambda^Z$ ,  $\lambda^\gamma$ , would enhance diboson production cross section and alter kinematic distributions. The limits on WWZ and WW $\gamma$  aTGC are derived by fitting the predicted leading lepton  $p_T$  spectrum as a function of aTGC values to the observed spectrum. The systematic uncertainties are incorporated in the fit using nuisance parameters with all correlations taken into account. Several constraining schemes are imposed on aTGC parameters to further reduce number of degrees of freedom in the fit. These are the "EQUAL", "LEP" and "HISZ" schemes [10]. To avoid tree-level unitarity violation at high centre-of-mass energies, the aTGC parameters are regularized using a form factor with a unitarisation energy scale [10].

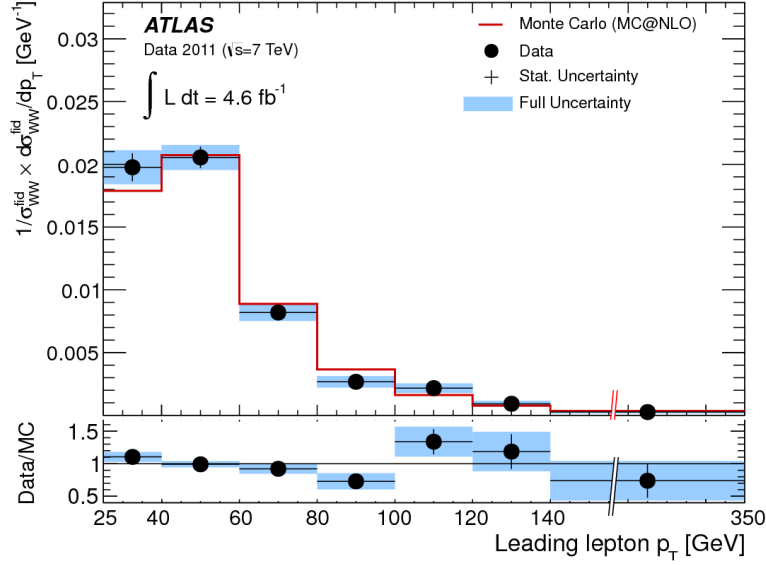


**Figure 1:** The normalized differential  $WW$  fiducial cross section as a function of the leading lepton  $p_T$  compared to the SM prediction [10].

The expected and observed 95% C.L. limits on  $WWZ$  and  $WW\gamma$  aTGC in the three constraining schemes and without any constrains for two unitarisation energy scales of  $\Lambda = 6$  TeV and  $\infty$  can be found in [10].

Figure 2 compares aTGC limits in the LEP constraining scheme with limits from the CMS [6], CDF [7], D0 [7] and LEP [8] experiments. Due to higher energy and the resulting higher  $WW$  production cross section at the LHC, the limits presented in this note are better than the Tevatron results and approach the precision of the combined limits from the LEP experiments.

### 3. Combined $WW$ and $WZ$ production in the semi-leptonic decay channel

The experimental signature of the combined  $WW$  and  $WZ$  production in the semi-leptonic final state consists in an electron or muon (denoted  $l$ ), two jets (denoted  $j_1, j_2$ ) and  $E_T^{miss}$ . The final states are splitted into two classes depending on the flavor of the final lepton (electron channel and muon channel).

The dominant background comes from the  $W/Z$ +jets processes. There are also contributions from multi-jet QCD processes, top production processes and  $WW/WZ$  diboson processes. The multi-jet QCD background is determined using a data-driven procedure where its shape and normalization are determined using two separate data control samples. The MC estimate of  $W/Z$ +jets background is normalized to data in a control region. All the other backgrounds are estimated fully using simulation.

The combined  $WW/WZ$  production cross section is extracted by performing a binned maximum-likelihood fit of the observed  $m_{jj}$  distribution of  $WW/WZ \rightarrow lvjj$  candidates. The parameter of interest in the fit is the ratio ( $\mu$ ) of the measured cross section over its NLO SM prediction. The leading sources of systematic uncertainty include limited signal MC statistics, jet energy scale and

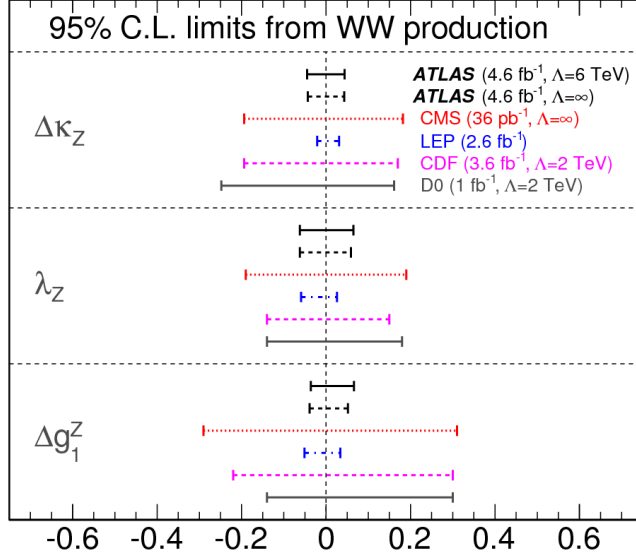


**Figure 2:** Comparison of anomalous TGC limits from ATLAS, CMS, CDF, D0 and LEP experiments for the LEP scenario [10].

resolution,  $W/Z$ +jets background normalization. The fitted  $\mu$  is  $1.13 \pm 0.34$  resulting in a measured total  $WW/WZ$  production cross section of  $72 \pm 9$  (stat.)  $\pm 15$  (syst.)  $\pm 13$  (MC stat.) pb, consistent with the predicted cross section of  $63.4 \pm 2.6$  pb.

More details concerning this analysis can be found in [15]

#### 4. Summary

$WW$  production cross section in 7 TeV pp collisions is measured with the ATLAS detector in both the total and fiducial phase spaces. The leptonic decays of  $WW$  pairs in a data set corresponding to a luminosity of  $4.7 \text{ fb}^{-1}$  are used. The reconstructed leading lepton  $p_T$  spectrum is unfolded and the normalized differential production cross section is extracted with respect to leading lepton  $p_T$ . The measured total cross section is  $51.9 \pm 2.0$  (stat.)  $\pm 3.9$  (syst.)  $\pm 2.0$  (lumi.) pb, consistent with the NLO SM prediction of  $44.7_{-1.9}^{+2.1}$  pb. aTGC limits are derived based on the observed spectrum. The obtained aTGC limits approach the precision of the combined limits from the four LEP experiments.

Combined  $WW/WZ$  production cross section is measured in the semi-leptonic final state of  $WW/WZ \rightarrow lvjj$  using the same data set. The measurement is performed by fitting the observed di-jet invariant mass distribution. The combined cross section is determined to be  $72 \pm 9$  (stat.)  $\pm 15$  (syst.)  $\pm 13$  (MC stat.) pb, in agreement with the predicted cross section of  $63.4 \pm 2.6$  pb

These diboson measurements are important tests of the electroweak theory in the SM and are among the groundwork for Higgs searches and studies and other new physics searches.

## References

- [1] L. Evans and P. Bryant (eds) JINST 3, S08001 (2008).
- [2] K. Hagiwara, S. Ishihara, R. Szalapski, and D. Zeppenfeld, Phys. Rev. D 48, 2182 (1993).
- [3] H. Davoudiasl, J. L. Hewett, and T. G. Rizzo, Phys. Rev. D 63, 075004 (2001); H. He et al., Phys. Rev. D 78, 031701 (2008).
- [4] ATLAS Collaboration, 2008 JINST 3 S08003
- [5] ATLAS Collaboration, Phys. Lett. B 712, 289 (2012).
- [6] CMS Collaboration, Phys. Lett. B 699, 25 (2011).
- [7] T. Aaltonen et al. (CDF Collaboration), Phys. Rev. Lett. 104, 201801 (2010); V. Abazov et al. (D0 Collaboration), Phys. Rev. Lett. 103, 191801 (2009); *ibid.*, Phys. Rev. D 80, 053012 (2009).
- [8] S. Schael et al. (ALEPH Collaboration), Phys. Lett. B 614, 7 (2005); J. Abdallah et al. (DELPHI Collaboration), Eur. Phys. J. C 54, 345 (2008); P. Achard et al. (L3 Collaboration), Phys. Lett. B 586, 151 (2004); G. Abbiendi et al. (OPAL Collaboration), Eur. Phys. J. C 33, 463 (2004).
- [9] CMS Collaboration, EPJC 73 (2013) 2283
- [10] ATLAS Collaboration, Phys. Rev. D 87, 112001 (2013)
- [11] J. M. Campbell, R. K. Ellis, and D. J. Rainwater, Phys. Rev. D 68, 094021 (2003).
- [12] P. M. Nadolsky et al., Phys. Rev. D 78, 013004 (2008).
- [13] G. D'Agostini, Nucl. Instr. Meth. A 362, 487 (1995).
- [14] K. Hagiwara, R. D. Peccei, D. Zeppenfeld, and K. Hikasa, Nucl. Phys. B 282, 253 (1987).
- [15] ATLAS Collaboration, ATLAS-CONF-2012-157, <http://cds.cern.ch/record/1493586>